

Stripe structure in the CuO_2 plane of perovskite superconductors

A. Bianconi, N. L. Saini, T. Rossetti, A. Lanzara, A. Perali, and M. Missori
Dipartimento di Fisica, Università di Roma "La Sapienza," Piazzale A. Moro 2, 00185 Roma, Italy

H. Oyanagi, H. Yamaguchi, and Y. Nishihara
Electrotechnical Laboratory, Umezono, Tsukuba, Ibaraki 305, Tsukuba, Japan

D. H. Ha

Korea Research Institute of Standards and Science, P.O. Box 3, Taedok, Taejeon 305-606, Korea
 (Received 28 May 1996)

The Cu-O pair-distribution function in a $\text{Bi}_2\text{Sr}_2\text{CaCu}_2\text{O}_{8+y}$ superconductor has been measured by polarized Cu K -edge extended x-ray-absorption fine structure at $T < T_c$. The results show an anomalous long Cu-O (planar) distance, 1.96 Å, assigned to distorted CuO_2 stripes of width W intercalated with undistorted stripes of width L . From the measurement of $L = 15 \pm 0.5$ Å we have calculated the energies E_n of the bottom of the one-dimensional subbands of the superlattice and found that the Fermi level E_F is tuned to a "shape resonance" $E_F - E_n < \hbar \omega_D$, where ω_D is the Debye frequency, giving the T_c amplification. [S0163-1829(96)04441-4]

$\text{Bi}_2\text{Sr}_2\text{CaCu}_2\text{O}_{8+y}$ (Bi-2212) has been selected in these last years as a test material to investigate the general properties of high- T_c superconductors such as the transport and magnetic properties,¹ the band structure, the superconducting gap, and its anisotropy.² It is formed by a stacked series of superconducting CuO_2 planes intercalated by nonsuperconducting BiO block layers. The three-dimensional (3D) phase coherence is provided by Josephson currents between layers.³ The solution of the incommensurate 1D superstructure of Bi-2212 with a large unit cell having five atomic species and a long wavelength (25 Å) is at the limit of the capabilities of diffraction methods, since a large number of parameters are needed in the structural refinement;⁴ and therefore its structure at the mesoscopic level is not well established.

The large displacive and substitutional one-dimensional superstructure of the nonsuperconducting BiO block layer is well established in the literature.⁴ It is common opinion that the superconducting CuO_2 plane is rigid, with constant CuO (planar) bond length 1.88 Å, and the weak modulation of the plane has little effect on its physical properties.

On the contrary a paradigm for understanding high- T_c superconductivity has been proposed based on a particular heterostructure of the CuO_2 plane at the mesoscopic scale.⁵⁻⁷ The CuO_2 plane has been found to be made of a superlattice of U stripes of width L of undistorted lattice, as that of the "average crystallographic" structure, forming the majority phase which are intercalated with a minority phase of D stripes of width W , with a distorted lattice having a different electronic structure. This heterostructure has been described as a superlattice SMSMSM of superconducting (S) and metal (M) stripes at a mesoscopic scale with $W < \xi_0$, where ξ_0 is the coherence length.^{6,7} The amplification of the critical temperature from the low ($T < 23$ K) to the high ($30 \text{ K} < T_c < 150$ K) temperature range is realized by tuning the Fermi level close to the bottom E_n of the quasi-one-dimensional (1D) subband n of this superlattice of quantum wires.⁷ This resonance is known as the "shape resonance" condition for elec-

trons at the Fermi level with wave vector $k_F \sim n\pi/L$. In fact in the frame of the standard BCS theory for superconductivity the effective electron-electron coupling is strongly enhanced when the Fermi level is close to a divergence in the quasi-1D density of states (DOS). Tuning the charge density (i.e., E_F) and/or the stripe width L (i.e., E_n) at the shape resonance in the narrow range $E_F - E_n < \hbar \omega_D$, where ω_D is the Debye frequency, gives a resonant amplification of the critical temperature in comparison with that of the homogeneous 2D plane.

In this experimental work we report results showing that the actual lattice distortions in the D stripes involve a large elongation of the in-plane Cu-O (planar) bonds that directly modifies the hopping integral in plane giving an electronic structure in the D stripes different from that in the U stripes. Moreover we report a more accurate measure of the width L of the U stripe that allows us to show that the shape resonance condition $E_F - E_n < \hbar \omega_D$ is verified at optimum doping.

The CuO_2 plane with the 1D aperiodic modulation shows an infinite number of different Cu site conformations of the CuO_5 pyramids that can be described by the statistical distribution of the Cu-O (planar) and the Cu-O (apical) distances. Here the distribution has been measured directly by Cu K -edge extended x-ray-absorption fine structure⁸⁻¹² (EXAFS) to overcome the limitations of the x-ray diffraction to solve the oxygen lattice structure. The polarized $\mathbf{E} \parallel \mathbf{a}$ and $\mathbf{E} \parallel \mathbf{c}$ Cu K -edge EXAFS experiments have been performed on Bi-2212 crystal to determine the statistical distribution of the Cu-O distances in the CuO_2 plane by this local (~ 5 Å) probe. The measurements were performed on the beam line BL-4C at the Photon Factory, Tsukuba.¹³ The spectra were recorded by detecting the fluorescence yield using 9 NaI(Tl) x-ray detectors. The crystal temperature was monitored with an accuracy of ± 0.5 K. The sample was a single crystal grown by the traveling floating-zone method¹⁴ with $T_c = 84$ K. The EXAFS signal $\chi = (\alpha - \alpha_0)/\alpha_0$, where α is the absorption coefficient and α_0 is the so called atomic absorption, was

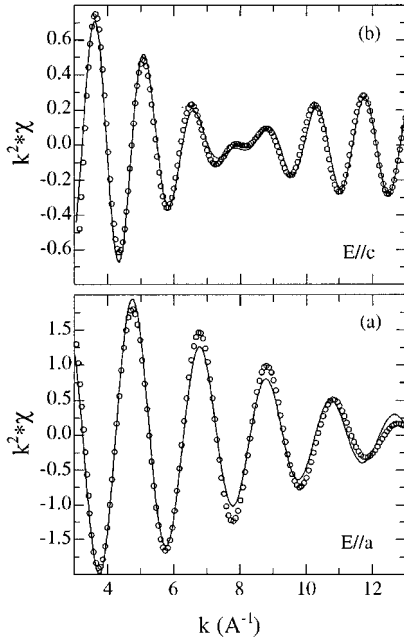


FIG. 1. Fourier-filtered first-shell experimental $\mathbf{E}\parallel\mathbf{a}$ Cu K -edge EXAFS signal (multiplied by k^2) due to the Cu-O (planar) pairs (circles) and its fit with two distances (solid line) at 30 K (a). Fourier-filtered first-shell experimental $\mathbf{E}\parallel\mathbf{c}$ Cu K -edge EXAFS signal due to the Cu-O (apical) pairs (squares) and its fit with two distances (solid line) at 30 K (b).

extracted from the absorption spectrum using standard procedure and corrected for fluorescence self-absorption.¹⁵

The signal due to the Cu-O (planar) [and Cu-O (apical)] is well isolated in the $\mathbf{E}\parallel\mathbf{a}$ [and $\mathbf{E}\parallel\mathbf{c}$] spectra. Figure 1 shows the Cu-O (planar) [and Cu-O (apical)] EXAFS signal obtained by standard Fourier filtering (between $k_{\min}=3 \text{ \AA}^{-1}$ to $k_{\max}=17 \text{ \AA}^{-1}$) from the $\mathbf{E}\parallel\mathbf{a}$ [and $\mathbf{E}\parallel\mathbf{c}$] Cu K -edge EXAFS. Multiple-scattering signals are not present because any multiple-scattering contribution will have a longer effective photoelectron pathway. The first-shell EXAFS data were fitted by nonlinear least-squares fitting using the curved wave EXAFS theory in the range $3\text{--}13 \text{ \AA}^{-1}$ where the EXAFS amplitude due to scattering by oxygen atoms is large. The results of the fitting show a distribution of different distances both in the plane and out of the plane. The number of independent parameters that can be extracted is $N_{\text{ind}}\sim(2\Delta k\Delta R)/\pi\sim 5$, where $\Delta k=10 \text{ \AA}^{-1}$ and $\Delta R=0.8 \text{ \AA}$, are the ranges in k and R space over which the first-shell data have been fitted. The best fits shown in Fig. 1 have been obtained by two shells fit with two distances R_{long} , R_{short} and effective coordination numbers N_{long} and $N_{\text{short}}=N_{\text{tot}}-N_{\text{long}}$ (where N_{tot} is fixed), the Debye-Waller factors were taken to be the same and it was found that they can be fixed to the expected values for the correlated Debye model. Thus the two distances fitting is essentially a three-parameters (R_{long} , R_{short} , and N_{long}) fit. All the other parameters were fixed to the values determined by using standard model compounds. A typical fit to the experimental $\mathbf{E}\parallel\mathbf{a}$ and $\mathbf{E}\parallel\mathbf{c}$ EXAFS is shown by a solid line in Fig. 1. The pair-distribution function (PDF) for the Cu-O pairs extracted from the data at 30 K is shown in Fig. 2. There is not a single Cu-O (planar) distance for the CuO_4 square planes but a wide distribution in the range $1.88\text{--}1.96 \text{ \AA}$. This range of variation is like that of the

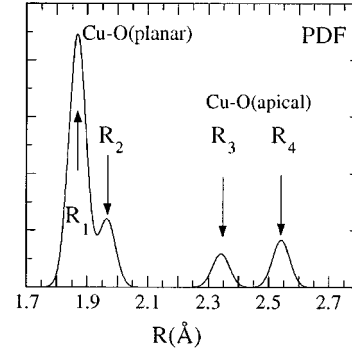


FIG. 2. Atomic pair-distribution function (PDF) from the central Cu for the square pyramids in Bi2212. The PDF of Cu-O (planar) pairs, obtained by $\mathbf{E}\parallel\mathbf{a}$ Cu K -edge EXAFS, show two Gaussians centered at R_1 and R_2 , normalized to $N(R_1)+N(R_2)=4$ and the Cu-O (apical) pairs obtained by $\mathbf{E}\parallel\mathbf{c}$ Cu K -edge EXAFS centered R_3 and R_4 normalized to $N(R_3)+N(R_4)=1$. The width of the Gaussians correspond to the correlated Debye-Waller factors [$\sigma^2=0.6\pm 0.2\times 10^{-3} \text{ \AA}^2$ ($0.8\pm 0.2\times 10^{-3} \text{ \AA}^2$) for in-plane (out-of-plane) oxygens].

average Cu-O (planar) distances in the crystallographic structures of all synthesized cuprate superconductors.¹⁶ The short Cu-O (planar) bonds at $R_1=1.88 \text{ \AA}$ are the expected distances for the average crystallographic structure. The long anomalous Cu-O (planar) bonds, $R_2=1.96 \text{ \AA}$ in Fig. 2 are associated with tilting of the CuO_4 square plane in the (110) direction, of the CuO_5 pyramids, where two oxygen atoms per CuO_4 square plane get displaced along the \mathbf{c} axis giving a rhombic distortion with two long distances R_2 and two short distances R_1 . We obtain the tilting angle $\theta=16^\circ$ (or $\theta=14^\circ$) of the CuO_4 square plane using $\cos\theta=R_1/R_2$ (or $\cos\theta=\langle R \rangle/R_2$, where $\langle R \rangle=a/\sqrt{2}$).

We can see directly the presence of two Cu-O (apical) distances $R_3=2.36 \text{ \AA}$ and $R_4=2.54 \text{ \AA}$ separated by $\Delta R\sim 0.18\pm 0.02 \text{ \AA}$ from the beat in the $\mathbf{E}\parallel\mathbf{c}$ EXAFS oscillations at $k\sim 8.5\pm 0.5 \text{ \AA}^{-1}$. The anomalous short Cu-O (apical) bonds R_3 are associated to the distorted CuO_5 pyramids.

From the PDF in Fig. 2 we obtain the probability $P_d=0.415$ for the minority distorted CuO_5 pyramids characterized by one Cu-O (apical)= R_3 , two Cu-O (planar)= R_1 and two Cu-O (planar)= R_2 and the probability $P_u=0.585$ for the majority undistorted CuO_5 pyramids characterized by one Cu-O (apical)= R_4 and four Cu-O (planar)= R_1 . The probability P_d is given by $N(R_3)/N_{\text{tot}}$ (from $\mathbf{E}\parallel\mathbf{c}$ data) $=2N(R_2)/N_{\text{tot}}$ (from $\mathbf{E}\parallel\mathbf{a}$ data); the probability $P_u=1-P_d=N(R_4)/N_{\text{tot}}$ (from $\mathbf{E}\parallel\mathbf{c}$ data). The measured probability P_u as a function of the temperature is reported in Fig. 3.

The spatial distribution of the distorted Cu sites and the measurement of the stripe width L has been obtained by joint EXAFS and diffraction experiments. The one-dimensional modulation of the Cu lattice has been determined by x-ray-diffraction anomalous diffraction at the Cu K edge. The experiment has been performed at the European Synchrotron Radiation Facility (ESRF, Grenoble, France) on the wiggler beam line ID 11-BL2.¹⁷ We report in Fig. 3 the measure of the wavelength λ of the 1D anharmonic modulation in the direction of the \mathbf{b} axis in the orthorhombic direction, at 45° from the Cu-O-Cu in the plane as a function of temperature. The large anharmonic character is indicated by the presence

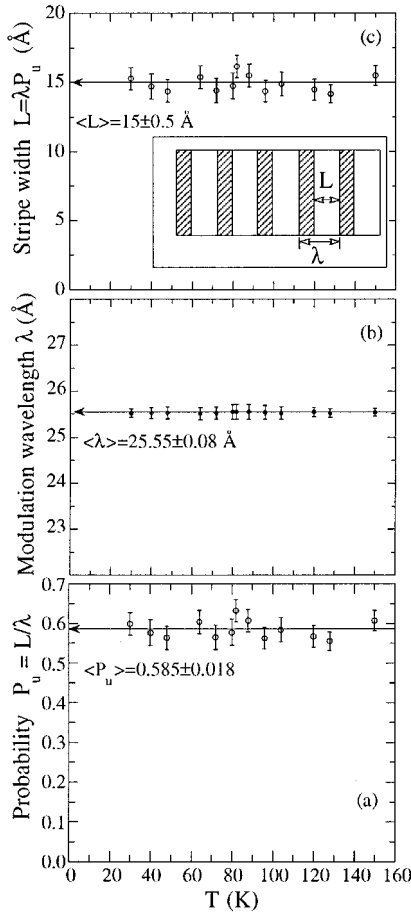


FIG. 3. Temperature dependence of the probability of the undistorted CuO_2 pyramids P_u given by $N(R_4)/[N(R_3) + N(R_4)]$ measured by $\mathbf{E}||\mathbf{c}$ EXAFS (a); the superstructure period λ measured by x-ray diffraction (b); the width L of the undistorted CuO_2 stripes given by $L = \lambda P_u = \lambda L/(L + W)$ (c), the pictorial view of the stripes in the CuO_2 plane is shown in the insert. The error bars on the mean values in the temperature range are 3σ .

of intense second-order diffraction peaks. The anharmonic modulation of the CuO_2 plane gives stripes of distorted lattice (D stripes) of width W that form linear domain walls intercalated with the stripes of undistorted lattice (U stripes) of width L ($L \neq W$) running along the \mathbf{a} -axis direction, as shown in the inset of Fig. 3(c). The probability of undistorted Cu sites in the U stripes is given by $P_u = L/(L + W)$ and the superstructure wavelength is $\lambda = W + L$. Therefore we have measured the width $L = \lambda P_u$ of undistorted lattice by joint EXAFS (P_u) and diffraction (λ) data that is plotted in Fig. 3 as a function of temperature. Previous measurements of L were obtained by λ measured by electron diffraction at room temperature with the assumption that λ is temperature independent, while in the present work λ and P_u are measured in the same temperature range on the same crystal providing the best accurate measurement of L .

This work shows that the lattice in plane distortions in the D stripes are large enough to give a local electronic structure different from the U stripes. In fact the elongation of the Cu-O (planar) bonds, by about 0.09 \AA , in the D stripes directly changes the hopping integral in the plane¹⁸ and modifies the band structure mainly at the M point of the Brillouin zone giving a potential barrier between the stripes. The large

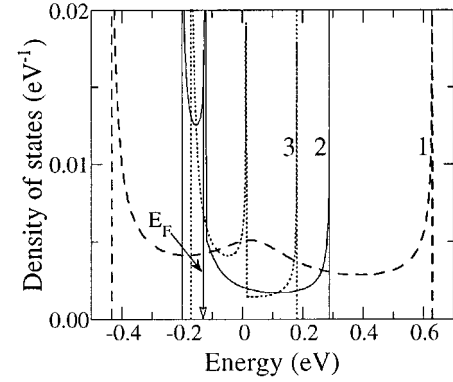


FIG. 4. The calculated density of states of the $n=1, 2,$ and 3 subbands for an ideal stripe of width $L=15 \text{ \AA}$ and infinite potential barrier, running in the (π, π) direction following the tetragonal notation for a square lattice. The position of the Fermi level E_F in Bi-2212 is indicated by an arrow.

tilting in the D stripes is expected to modify the electronic structure and following Ref. 19 to suppress the critical temperature. Therefore the electronic structure of the modulated CuO_2 plane can be described as a superlattice of quantum wires with the formation of superlattice subbands.²⁰ We analyze the electronic structure of this system with a simplified model assuming an infinite potential barrier between the stripes, and so an electron wave vector in the y direction (perpendicular to the stripes) quantized $k_y(n) = n\pi/L$. For each integer value n , a one-dimensional (1D) subband is defined with energy minima E_n that depends on the actual electron effective mass, i.e., on the band dispersion. Recently a phenomenological tight-binding fit of the experimental band dispersion has provided the hopping coefficients for the CuO_2 band of Bi-2212,² that we have used for evaluation of subbands and the relative density of states. Each 1D subband (n) is obtained by cutting the 2D dispersion with fixed $k_y(n) = n\pi/L$, where $L=15 \pm 0.5 \text{ \AA}$ is given by the present experiment. The resulting density of states (DOS) for the first three subbands is shown in Fig. 4. The Fermi level is near to the divergence of the DOS in the second subband, and it is separated from its bottom by $(E_F - E_2) \sim 70 \text{ meV}$, moreover it is close the bottom of the third subband $(E_F - E_3) \sim 40 \text{ meV}$, therefore the shape resonant condition is verified with $E_F - E_n < \hbar\omega_D$, where $\hbar\omega_D \sim 50 \text{ meV}$. From this result follows that the critical temperature of the homogeneous 2D plane is amplified by a large factor²⁰ from the low to the high temperature range.

The spots on the Fermi surface for an ideal single quantum wire are identified by the crossing of the lines of constant $k_y(n)$. We have plotted, in Fig. 5, the Fermi surface deduced by angle-resolved photoemission data for a Bi-2212 crystal.² We see that the second subband is characterized by two pairs of spots $\mathbf{k}_1, \mathbf{k}'_1, \mathbf{k}_2,$ and \mathbf{k}'_2 on the Fermi surface such that $k_1 - k'_1 \sim G + q$, where G is the antiferromagnetic lattice vector $G = 2\pi/a$ ($a = d\sqrt{2}$, where d is the Cu-Cu distance) and where q is a small transfer wave vector. The Fermi spots of the third subband satisfy a similar relation. In this landscape the electron pair with wave vectors $(\mathbf{k}_1, \mathbf{k}_2)$ get scattered in $(\mathbf{k}'_1, \mathbf{k}'_2)$ with an exchanged momentum $Q = G + q$ involving mainly the small transfer wave vector q in the pairing mechanism for changes in the U stripes medi-

ated by magnetic fluctuations in the D stripes. Moreover the anomalous linear temperature dependent resistivity in the cuprate superconductors at optimum doping can be explained if the Fermi surface is limited to these hot spots.²¹

The angular-resolved photoemission (ARPES) of Bi-2212 shows anomalous behavior if interpreted without taking into account the modulation of the CuO_2 plane. An enhancement of the photoelectron intensity has been reported at the spots predicted here²² that are even more clear at higher binding energy suggesting the deviation from the dispersion expected for a homogeneous 2D lattice. Quantitative comparison of ARPES with the predicted electronic structure requires the calculation of the actual subbands for the superlattice. The density of states for the superlattice depends on the interface width and distortions, the potential barrier, the hopping between neighboring stripes, the electron effective mass, etc. All these effects are expected to give broadening to the ideal density of states calculated for a single stripe and infinite potential barrier as shown in Fig. 4. However the Fermi level is expected to remain close to a divergence in the 1D-DOS.

In summary, we have measured the Cu-O distances of the distorted CuO_5 pyramids in the Bi-2212 system showing an elongation of the Cu-O (planar) bonds R_2 relevant for the electronic structure of the CuO_2 plane. The accurate measurement of the width $L=15\pm 0.5$ Å of the undistorted stripes by joint x-ray diffraction and EXAFS has allowed us to calculate the quasi-one-dimensional density of states and to show that the Fermi level is tuned to a 1D "shape resonance" that gives the amplification of the critical temperature from the low-temperature range $T_c < 23$ K of an homogeneous plane to the high-temperature range $23 < T_c < 150$ K.²⁰

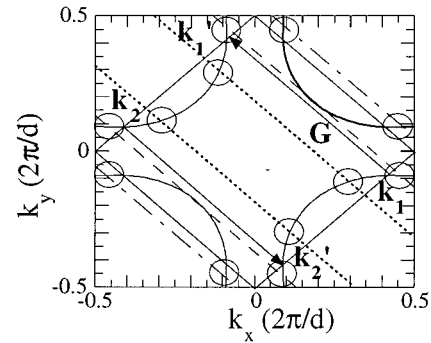


FIG. 5. Hot spots on the Fermi surface are identified by the crossing points between the Fermi surface for an homogeneous 2D CuO_2 plane with 0.16 holes per Cu site and lines with constant wave vector $k_y(n) = n\pi/L$ [$n=1$ (dotted lines), $n=2$ (dashed lines), and $n=3$ (dot-dashed lines)], where $L=15$ Å is the width of the U stripes. The wave vectors k_x and k_y are measured in units of $2\pi/d$, where d is the Cu-Cu distance. \mathbf{G} is the antiferromagnetic vector $G=2\pi/a$ with $a=d\sqrt{2}$.

The presence of stripes of distorted lattice seems to be a general characteristic of the cuprate superconductors in fact they have been recently found in $\text{La}_{1.85}\text{Sr}_{0.15}\text{CuO}_4$,²³ and in the metallic superconducting oxygen doped $\text{La}_2\text{CuO}_{4+y}$.²⁴

This work was partially funded by Istituto Nazionale di Fisica della Materia, Istituto Nazionale di Fisica Nucleare, Consiglio Nazionale delle Ricerche, and Centro Internazionale di Fisica Teorica di Trieste. We thank M. Lusignoli, P. Bordet, A. Kvik, and P. Radaelli for help in the x-ray-diffraction work.

¹A. Maeda *et al.*, Phys. Rev. B **41**, 6418 (1990).

²M. R. Norman *et al.*, Phys. Rev. B **52**, 615 (1995), and references cited therein.

³P. Müller, in *Festkörperprobleme/Advances in Solid State Physics*, edited by R. Helbig (Vieweg, Braunschweig 1994), Vol. 34, p. 1.

⁴E. A. Hewat *et al.*, Nature (London) **333**, 53 (1988); Y. Gao *et al.*, Science **241**, 954 (1988); G. Calestani *et al.*, Physica C **161**, 598 (1989); V. Petricek *et al.*, Phys. Rev. B **42**, 387 (1990); X. B. Kan and S. C. Moss, Acta Crystallogr. B **48**, 122 (1992); A. Yamamoto *et al.*, Phys. Rev. B **42**, 4228 (1990); A. I. Beskrovnyi *et al.*, Physica C **166**, 79 (1990); **171**, 19 (1990).

⁵A. Bianconi, in *International Conference on Superconductivity*, edited by S. K. Joshi *et al.* (World Scientific, Singapore, 1990), p. 448; A. Bianconi *et al.*, in *Lattice Effects in High- T_c Superconductors*, edited by Y. Bar-Yam *et al.* (World Scientific, Singapore, 1992), p. 65.

⁶A. Bianconi *et al.*, Europhys. Lett. **31**, 411 (1995); M. Missori *et al.*, Physica C **235-240**, 1245 (1994).

⁷A. Bianconi and M. Missori, J. Phys. I (France) **4**, 361 (1994); A. Bianconi, Solid State Commun. **89**, 933 (1994); Physica C **235-240**, 269 (1994); A. Bianconi *et al.*, J. Supercond. **8**, 545 (1995).

⁸*X Ray Absorption: Principle, Applications Techniques of EXAFS, SEXAFS and XANES*, edited by R. Prinz and D. Koningsberger (Wiley, New York, 1988).

⁹J. B. Boyce *et al.*, Phys. Rev. B **35**, 7203 (1987); Phys. Scr. **37**, 912 (1988).

¹⁰J. Mustre de Leon, Phys. Rev. B **47**, 12 322 (1993), and references therein.

¹¹J. Röhler, in *Materials and Crystallographic Aspects of HTc-Superconductivity*, edited by E. Kaldis (Kluwer, Netherlands, 1994), p. 353.

¹²H. Yamaguchi *et al.*, Physica C **213**, 375 (1993), and references cited therein.

¹³H. Oyanagi *et al.*, Jpn. J. Appl. Phys. **24**, 610 (1985).

¹⁴D. H. Ha *et al.*, in *Advances in Superconductivity V*, edited by Y. Bando and H. Yamauchi (Springer-Verlag, Tokyo, 1993), p. 323.

¹⁵L. Tröger *et al.*, Phys. Rev. B **46**, 3283 (1992).

¹⁶H. Ihara, in Proceedings of ETL Workshop on High Temperature Superconductors [Bull. Electrochem. Lab. **58**, 64 (1994)].

¹⁷A. Bianconi *et al.*, Phys. Rev. B **54**, 4310 (1996).

¹⁸Y. Seino *et al.*, J. Phys. Soc. Jpn. **59**, 815 (1990).

¹⁹B. Büchner *et al.*, Phys. Rev. Lett. **73**, 1841 (1994).

²⁰A. Perali *et al.*, Solid State Commun. **100**, 181 (1996).

²¹R. Hlubina and T. M. Rice, Phys. Rev. B **51**, 9253 (1995).

²²J. Osterwalder *et al.*, Appl. Phys. A **60**, 247 (1995).

²³A. Bianconi *et al.*, Phys. Rev. Lett. **76**, 3412 (1996).

²⁴P. C. Hammel *et al.*, Phys. Rev. Lett. **71**, 440 (1993); P. G. Radaelli *et al.*, Phys. Rev. B **48**, 499 (1993).